




Case Report

Horizontal Guided Bone Regeneration Using Titanium-Reinforced Dense PTFE Membrane and Synthetic Nanocrystalline Hydroxyapatite: A Case Study Reporting Clinical and Histological Outcomes with 5-Year Follow-Up

Fabrizio Belleggia ^{1,*}, Luca Signorini ¹, Mirko Martelli ²  and Marco Gargari ²

¹ School of Dental Medicine, Saint Camillus International University of Health and Medical Sciences, Via di S. Alessandro 8, 00131 Rome, Italy

² School of Dental Medicine, "Ospedale San Pietro FBF", University of Rome "Tor Vergata", Via Cassia 600, 00189 Rome, Italy

* Correspondence: fabriziobelleggia@virgilio.it

Abstract: Background/Objectives: Guided bone regeneration (GBR) is a regenerative technique used to treat maxillary osseous defects to enable implant placement for prosthetic rehabilitation. It is generally performed with the use of barrier membranes and bone substitute materials of human or animal origin. Here, we report the clinical and histological outcomes of a horizontal GBR, treated using only synthetic biomaterials. **Methods:** A graft of nanocrystalline hydroxyapatite (NH) embedded in a silica gel matrix was used to fill a horizontal bone defect. The graft was covered with a titanium-reinforced dense polytetrafluoroethylene (TR-dPTFE) membrane, and primary closure was completed and maintained for 10 months. Then, the site was re-opened for membrane removal and implant insertion. During implant bed preparation, a bone biopsy was obtained for histological evaluation. A metal–ceramic crown was fitted, and the 5-year follow-up after prosthetic loading showed clinical and radiographically healthy tissues. **Results:** Histological examination revealed good integration of the biomaterial into the surrounding tissues, which were composed of lamellar bone trabeculae and connective tissue. New bone formation occurred not only around the NH granules but even inside the porous amorphous particles. **Conclusions:** The combination of NH and the TR-dPTFE membrane produced good clinical and histological results, which remained stable for 5 years.

Keywords: biocompatible materials; bone replacement materials; guided bone regeneration; horizontal defect; nanocrystalline hydroxyapatite; silica gel matrix; titanium-reinforced dense polytetrafluoroethylene membrane



Academic Editor: Pier Paolo Claudio

Received: 29 April 2025

Revised: 22 May 2025

Accepted: 28 May 2025

Published: 31 May 2025

Citation: Belleggia, F.; Signorini, L.; Martelli, M.; Gargari, M. Horizontal Guided Bone Regeneration Using Titanium-Reinforced Dense PTFE Membrane and Synthetic Nanocrystalline Hydroxyapatite: A Case Study Reporting Clinical and Histological Outcomes with 5-Year Follow-Up. *Int. J. Transl. Med.* **2025**, *5*, 19. <https://doi.org/10.3390/ijtm5020019>

Copyright: © 2025 by the authors. Licensee MDPI, Basel, Switzerland. This article is an open access article distributed under the terms and conditions of the Creative Commons Attribution (CC BY) license (<https://creativecommons.org/licenses/by/4.0/>).

1. Introduction

Guided bone regeneration (GBR) is a valid option to treat localized bone defects of the alveolar crest caused by trauma or the extraction of teeth with fractured roots, periapical lesions, or advanced periodontal disease [1].

This technique is based on the use of a membrane that acts as a physical barrier when applied over bone defects, creating a secluded space that facilitates the proliferation of angiogenic and osteogenic cells from the marrow space into the defect, preventing the ingrowth of competing, nonosteogenic cells into the membrane-protected space [2,3]. Membranes can be classified according to their origin—natural or synthetic—and whether they are resorbable or non-resorbable [4].

In order to create and maintain space, these membranes need to be supported by the appropriate bone fillers to avoid membrane collapse [5]. Bone grafts and bone substitutes of different origins have been successfully used beneath the membranes [6]. Although autogenous bones are considered the gold standard of grafting materials, due to its osteogenic, osteoinductive, and osteoconductive properties, important drawbacks include donor site morbidity, limited availability, and fast resorption rate.

Allografts and xenografts possess good osteoconductive properties. However, depending on the human or animal source, patients might raise objections concerning the risk of cross-infection, disease transmission, or religious concerns. For these reasons, alloplastic materials are increasingly utilized by researchers to develop effective synthetic bone substitute materials (BSMs), typically bioceramics based on calcium phosphate, such as hydroxyapatite (HA), β -tricalciumphosphate (β -TCP), or calcium sulphate [6]. These biomaterials have only osteoconductive properties, undergo complete resorption, do not present a risk of cross-infection—thanks to their synthetic origin—and offer unlimited availability. Bone grafts are usually composed of a mixture of autologous bone, for its osteogenic and osteoinductive properties, and a BSM [7], for its greater long-term stability, osteoconductive properties, and for the fact that it reduces the quantity of autologous bone, which very often requires the opening of a donor surgical site, increasing costs, the duration of the operation, and the post-operative discomfort of the patient.

The aim of this report is to evaluate, clinically and histologically, the use of a non-sintered bioceramic composed of nanocrystalline hydroxyapatite (NH) embedded in a silica gel matrix, covered by a titanium-reinforced dense polytetrafluoroethylene (TR-dPTFE) membrane, in a horizontal GBR procedure. A non-resorbable synthetic membrane was chosen for its unlimited barrier function over time, and the combination with an alloplast made it a completely synthetic augmentation procedure, without the use of autologous bone or biomaterials of human or animal origin, since information about this procedure is scarce in humans. To the best of the authors' knowledge, this is the first case reported in the literature exhibiting the association of these two biomaterials.

2. Materials and Methods

A 22-year-old healthy, non-smoker female patient presented with a chief complaint of recurrent infections of the first maxillary left molar due to a large osteolytic lesion caused by the failure of repeated endodontic therapies, as revealed by computed tomography (CT) scans (Figure 1A,B).

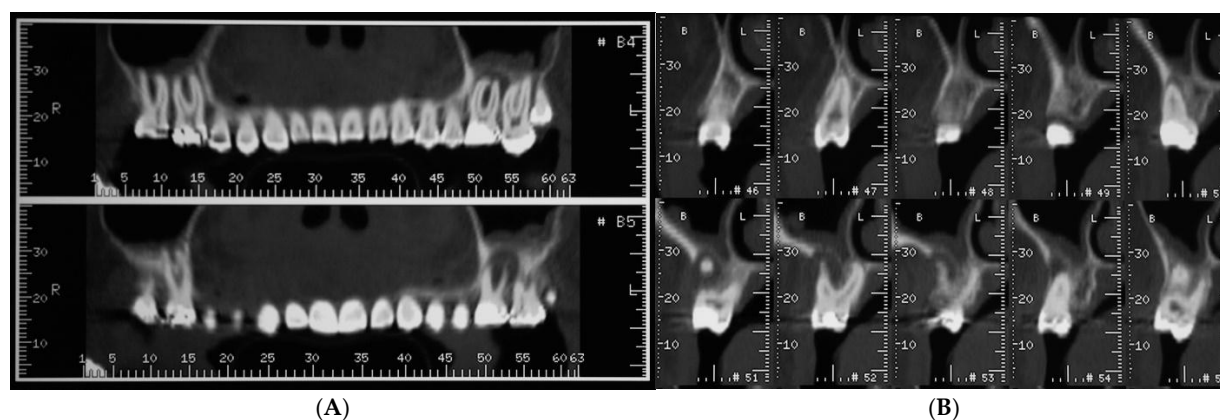


Figure 1. Computed tomography (CT) scans revealed large osteolytic lesion of first maxillary left molar caused by failure of repeated endodontic therapies (A). Cross-sections showing buccal bone loss (B).

Treatment options were discussed, and the patient signed a consent form for the tooth extraction and the subsequent augmentation procedure, to be scheduled as a staged approach for implant site development. Four months after the tooth extraction, soft tissue healing reached a proper maturation (Figure 2A,B), and a new CT was requested to evaluate the wound healing and bone availability for implant therapy. The CT scans revealed a horizontal ridge defect (Figure 2C,D–F) that required correction with a staged GBR procedure.

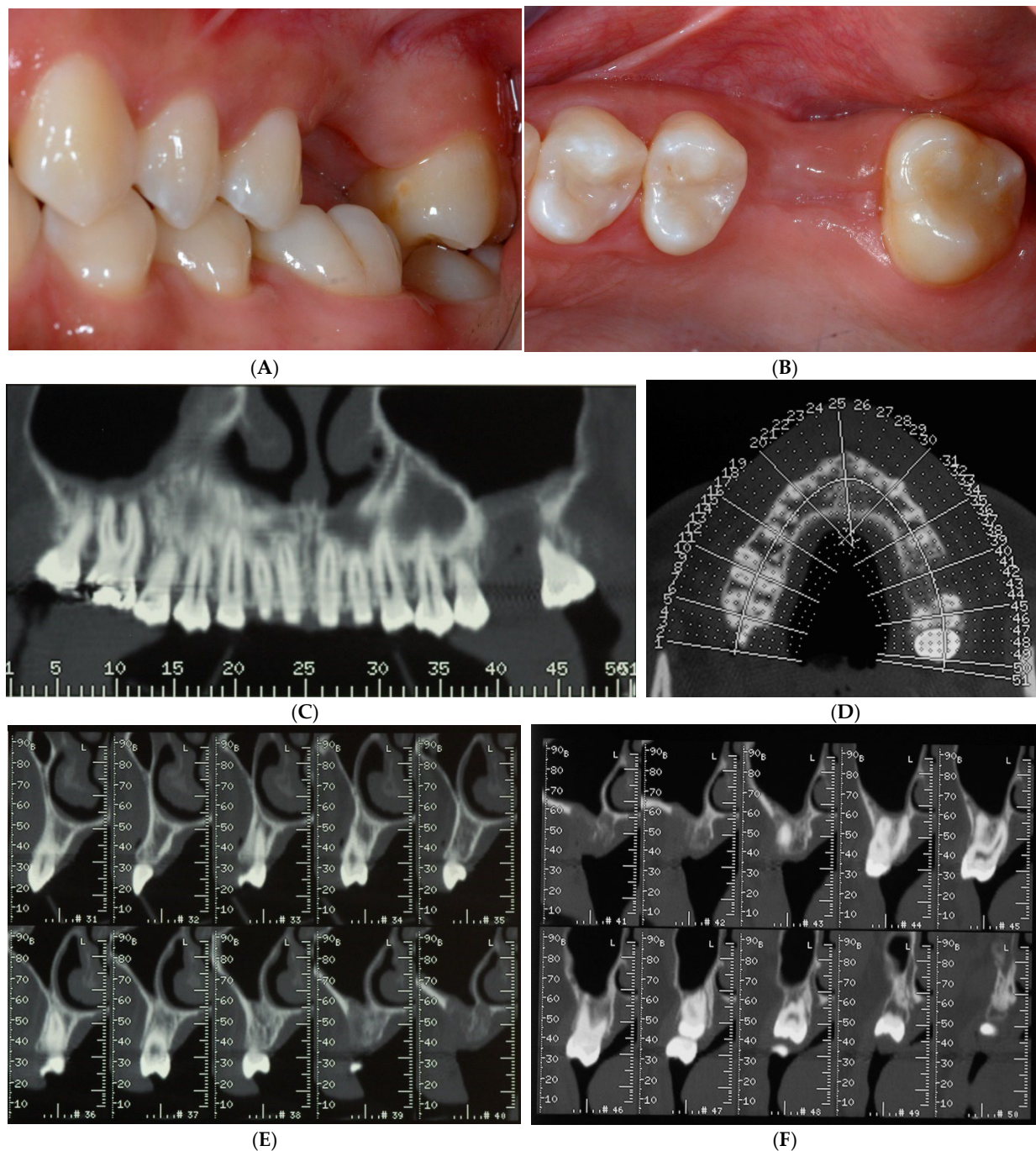


Figure 2. Soft tissue healing four months after tooth extraction (A,B). New CT was requested to evaluate wound healing and current bone availability for implant therapy. CT scans revealed horizontal ridge defect (C–F) that had to be corrected with a regenerative procedure.

After making the crestal incision, two vertical buccal releasing incisions—mesial to the second premolar and distal to the second molar—were performed. Then, a mucoperiosteal flap was raised, revealing the wide ridge deficiency (approximately 5, 7, and 9 mm in the mesio-distal, bucco-palatal, and corono-apical directions, respectively), highlighting the impossibility of achieving proper implant stability (Figure 3A,B). Then, a copious bleeding recipient site was created by bur perforations through the medullary spaces. A TR-dPTFE membrane (Cytoplast[®] Ti 250 Buccal, Osteogenics Biomedical, Lubbock, TX, USA) was shaped and trimmed with scissors to fit the ridge defect (Figure 4A), taking care to position the membrane edges 1.5 mm away from the adjacent roots, and stabilized with two pins on the buccal side. A graft of 100% NH embedded in a silica gel matrix (NanoBone[®] Artoss, Rostock, Germany), in the form of 0.6 × 2 mm granules, wetted with sterile saline (Figure 4B), was applied and compacted with a spoon/plugger tool to avoid leaving voids, but without over-compacting the material (Figure 4C). The membrane was moved to the palatal side and stabilized with an additional pin to the palatal bone wall (Figure 4D,E). A continuous periosteal incision along the entire length allowed the buccal flap to move coronally, followed by tension-free suturing using horizontal mattress and single stitches (Figure 5A) with PTFE material (Cytoplast[®] suture, Osteogenics Biomedical, Lubbock, TX, USA), which were removed 14 days later (Figure 5B). Healing was uneventful, and after a period of 10 months (Figure 6A–C), the site was re-opened for membrane removal and implant insertion. A smaller paramarginal trapezoidal mucoperiosteal flap, sparing the periodontum of the adjacent teeth, was raised (Figure 6D,E). The membrane was easily removed, and the defect appeared to be completely regenerated (Figure 6F). A 4 mm wide trephine bur (Stoma[®], Emmingen-Liptingen, Germany) was used to harvest a bone biopsy (Figure 7A), measuring 3 mm in diameter and about 6 mm in length (Figure 7B), so as not to extend the future implant bed preparation. The implant bed was then definitively prepared with the drill dedicated to the chosen implant (Figure 7C), a 5.0 × 9 mm implant (Camlog[®] Screw Line Promote Plus Biotechnologies, Basel, Suisse). The bone biopsy was immediately fixed in 10% neutral buffered formalin and stored at room temperature. The specimen was then decalcified in formic acid, dehydrated in progressively more concentrated ethanol, and finally embedded in paraffin. Sections of 5–6 µm thickness were cut with a microtome (Leica SM 2.400, Solms, Germany) and stained with hematoxylin and eosin and the Azan–Mallory staining technique for light microscopy. Histological evaluation and photo documentation were performed using the Axiophot microscope (Zeiss, Göttingen, Germany) at 12.5×, 25×, 100×, 200×, 400× magnifications.

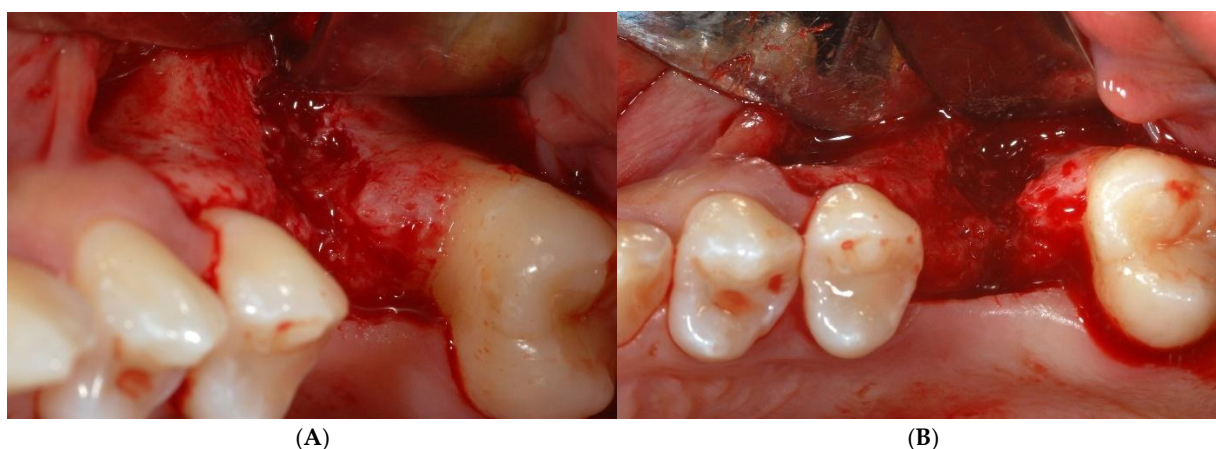


Figure 3. After buccal flap reflection with two vertical releasing incisions, wide horizontal bone defect was evident (A,B).

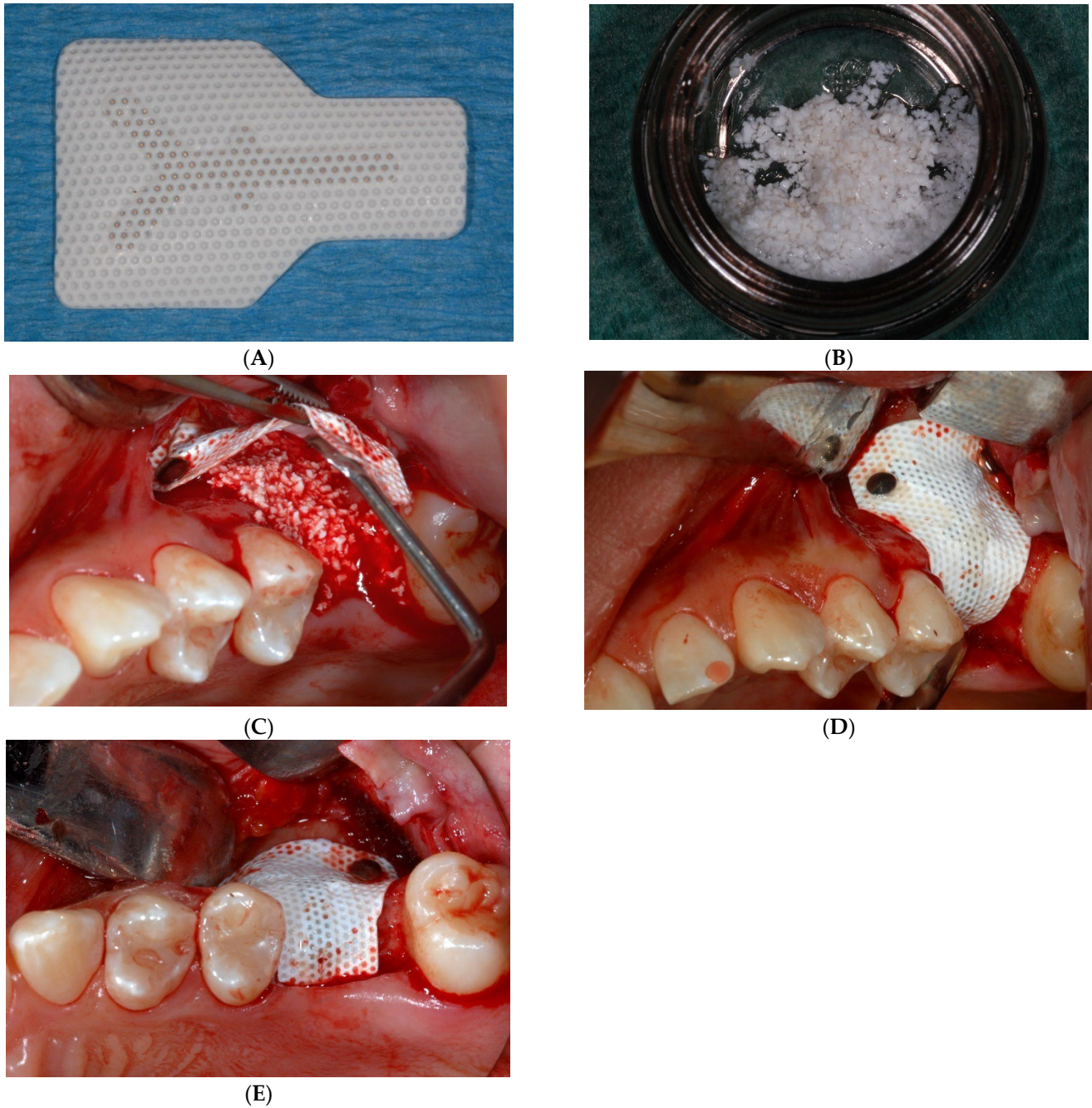


Figure 4. Titanium-reinforced dense polytetrafluoroethylene (TR-dPTFE) membrane was shaped and trimmed with scissors to fit ridge defect (A) and stabilized with 2 pins on buccal side. Particulate graft of 100% nanocrystalline hydroxyapatite (NH) embedded in a silica gel matrix, wetted with sterile saline (B), was packed to fill defect (C). Membrane was moved to the palatal side and stabilized with additional pin to palatal bone wall (D,E).

After implant insertion (Figure 7D), a healing abutment was immediately connected (Figure 7E) for transmucosal healing, avoiding additional surgery. After a 2-month healing time (Figure 7F), a provisional restoration was applied for progressive loading. At 6 months after implant insertion, a definitive porcelain-fused-to-metal crown was cemented (Figure 8A–C).

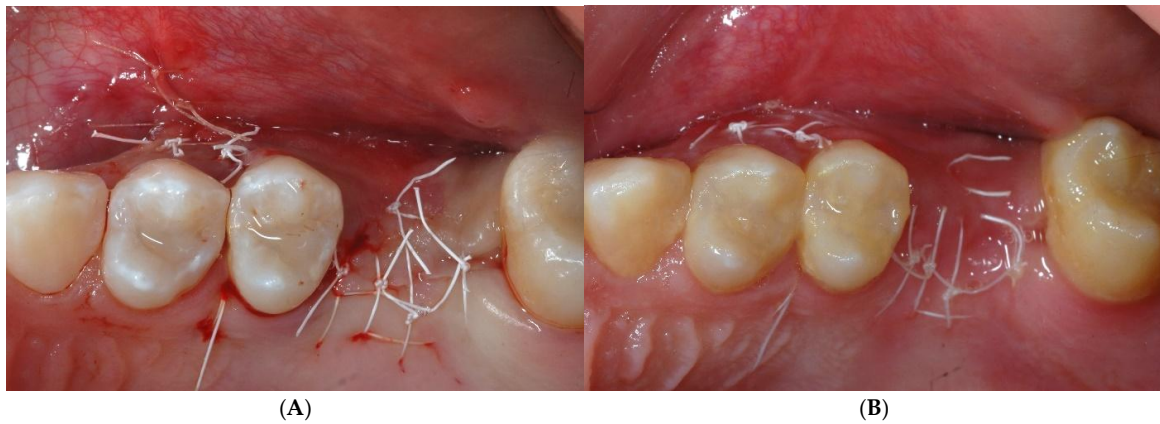


Figure 5. Tension-free suture with horizontal mattress and single PTFE stitches was obtained (A). Sutures were removed 14 days later (B).

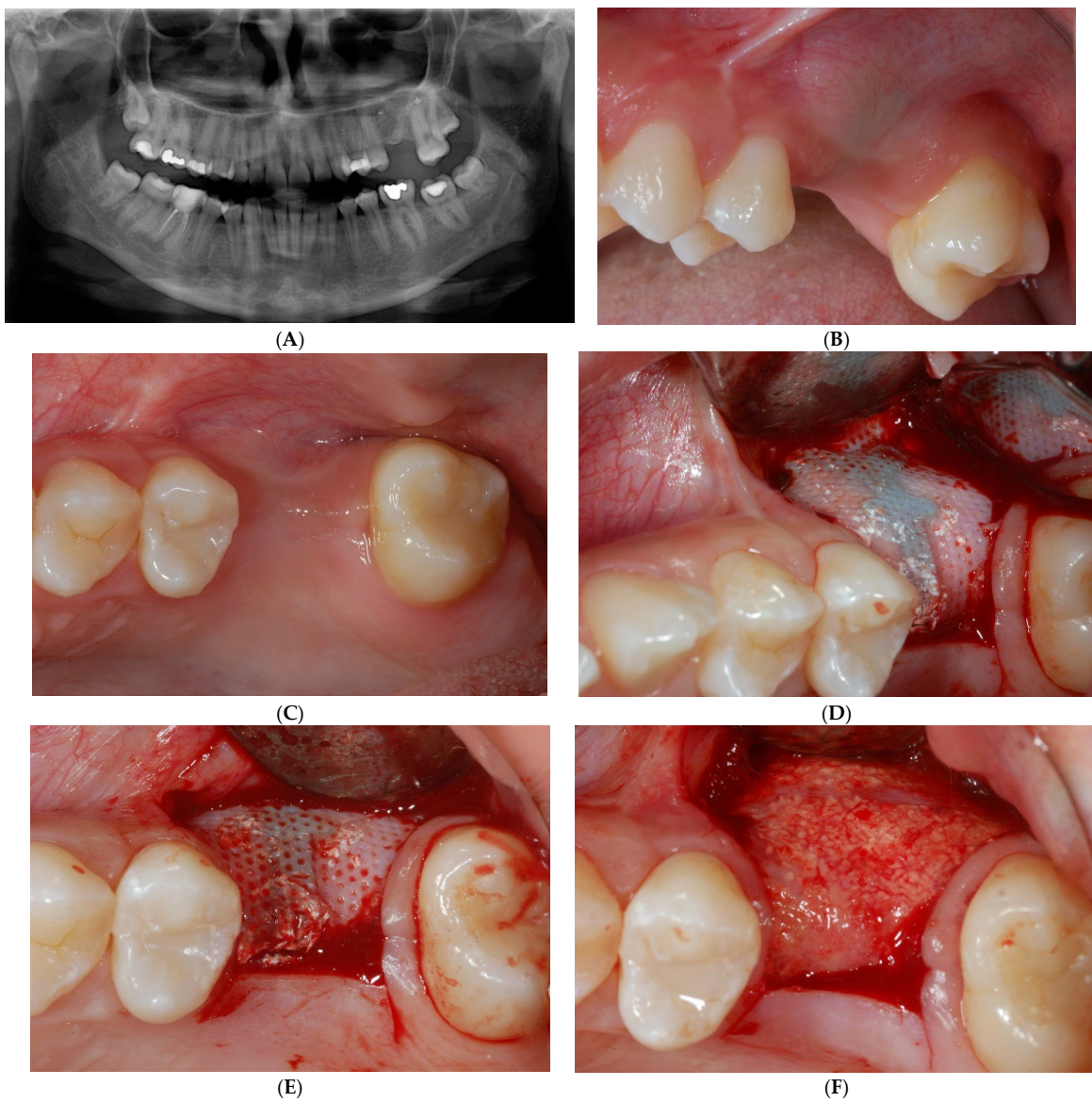


Figure 6. Radiographic (A) and clinical (B,C) follow-up after a 10-month healing period. Site was re-opened for membrane removal and implant insertion. Smaller paramarginal trapezoidal mucoperiosteal flap, sparing the periodontum of adjacent teeth, was raised (D,E). Membrane was easily removed, and defect appeared completely regenerated (F).

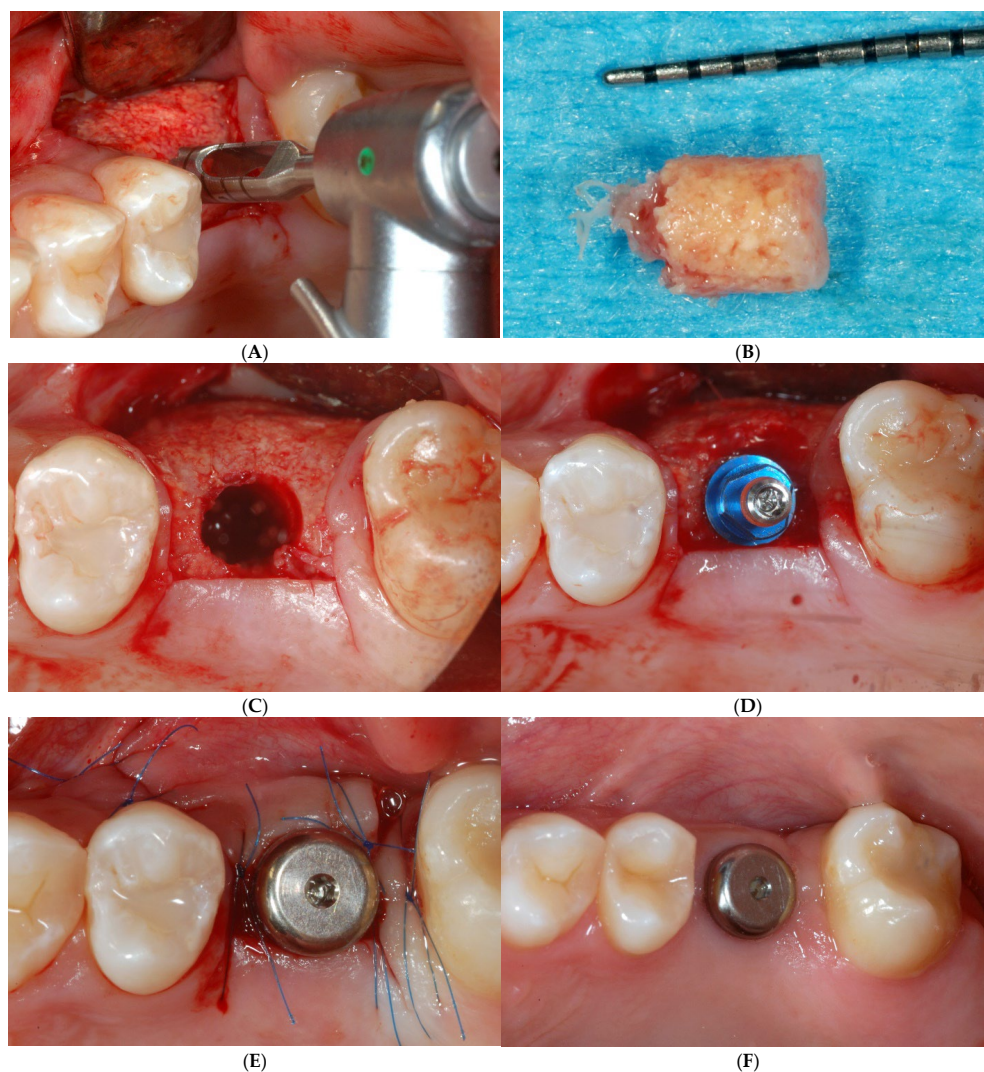


Figure 7. Trephine bur was used to harvest bone biopsy (A), measuring 3 mm in diameter and about 6 mm in length (B), during implant bed preparation (C). After implant insertion (D), a healing abutment was immediately connected (E) for transmucosal healing, avoiding additional surgery. Healing was uneventful and 2 months later (F), site was ready for prosthetic rehabilitation.

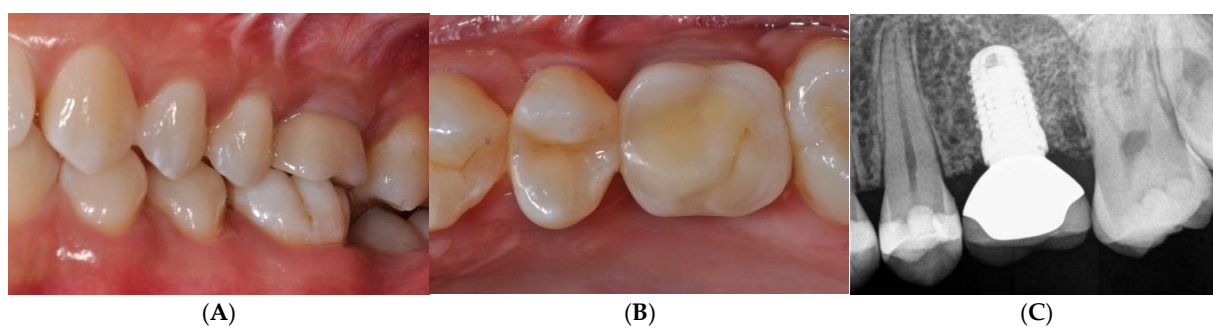


Figure 8. Provisional restoration was applied for progressive loading. At 6 months after implant insertion, a definitive porcelain-fused-to-metal crown was cemented (A–C).

3. Results

This GBR procedure was effective for the reconstruction of the horizontal defect, and the bone underneath the TR-dPTFE membrane appeared well mineralized after a healing period of 10 months. The implant was inserted in well-matured and vascularized bone and

achieved primary stability very easily. No additional ridge augmentation was required for implant placement. Regenerated bone was found to be uniform across the defect and was hard and well integrated. The patient was very satisfied with the aesthetic result of the prosthetic rehabilitation and the improved masticatory function. She was monitored at least twice a year, when she returned for professional hygiene sessions. There were no problems of peri-implantitis, unscrewing of the implant abutment screw or soft tissue recession. The 5-year clinical and radiographic follow-up after functional prosthetic loading showed the augmented hard and soft tissues well maintained, with no marginal bone loss around the implant and a bone density within the limits (Figure 9A,B).

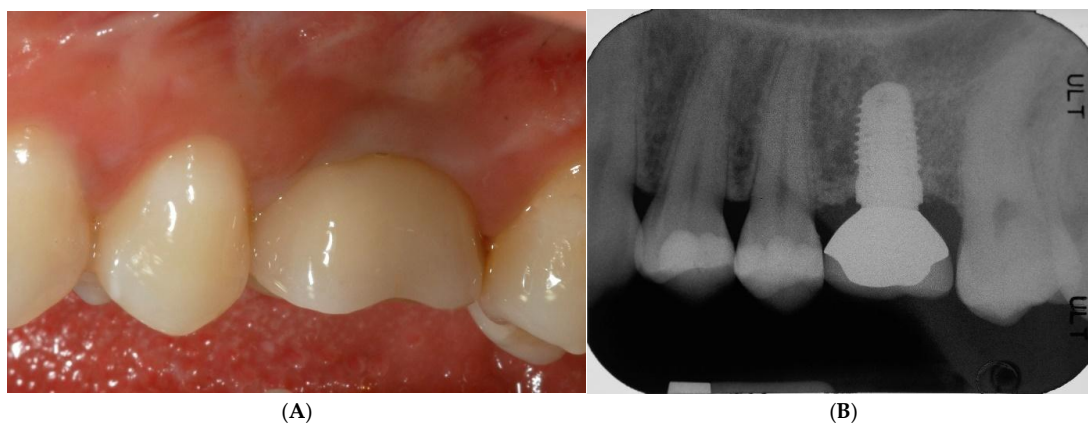


Figure 9. 5-year clinical (A) and radiographic (B) follow-up after functional prosthetic loading showed augmented hard and soft tissues, which were well maintained.

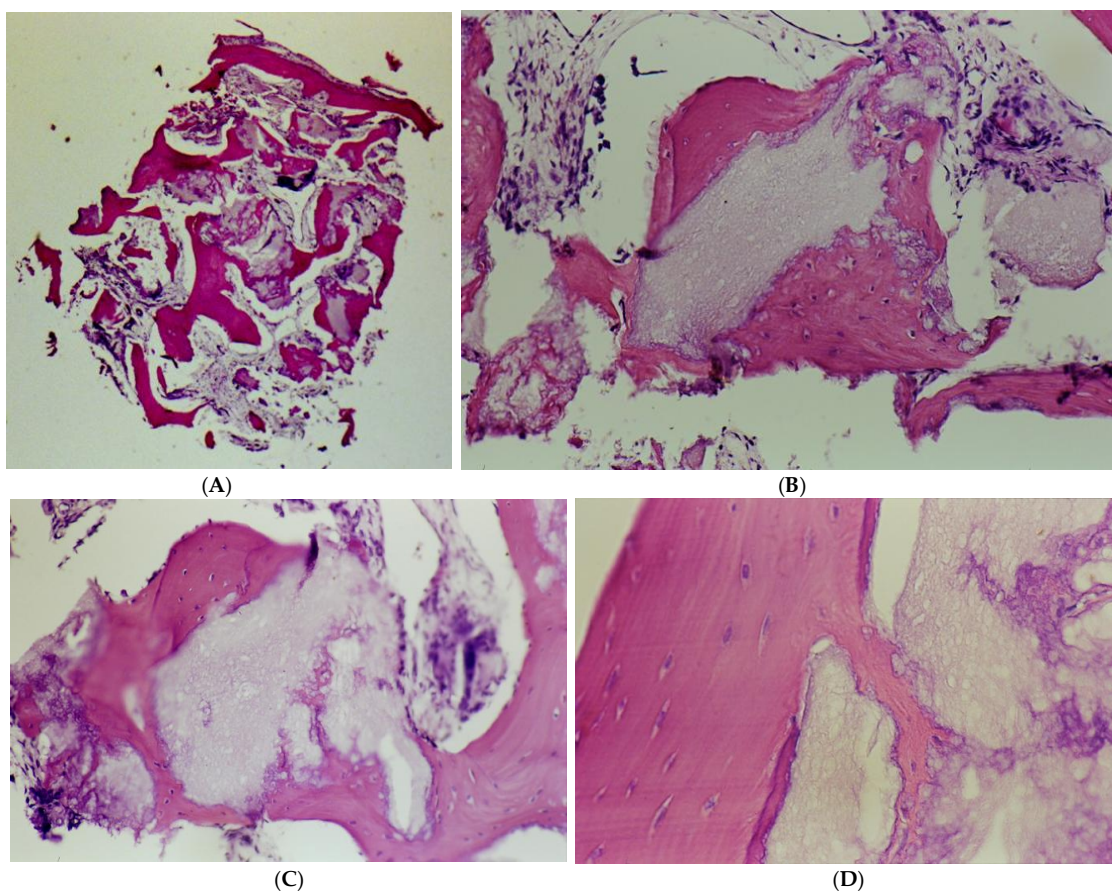


Figure 10. Light microscopic analysis revealed new bone formation throughout all parts of biopsy, with homogeneous presence of trabecular bone structures in intimate contact with surface of NH granules,

and marrow spaces with loose, highly vascularized connective tissue. There was no evidence of inflammation or foreign body reaction around NH remnants. The bone structure consisted mostly of newly formed mature lamellar bone, with Haversian systems, cement lines, and osteocytes, highlighting vitality of bone tissue. Non-degraded NH granules appeared structurally porous and inhomogeneous, were partially surrounded by osteoid or woven bone, and were lined with seams of osteoblasts. Osteoid protrusion and extension into graft material were observed. Fibrovascular extension with osteoid deposition within nanostructured porous granule was observed, composed of cellular fibrous connective tissue undergoing mineralization, creating an arboreal network. Hematoxylin and eosin staining, magnification 25× (A), 200× (B,C), 400× (D).

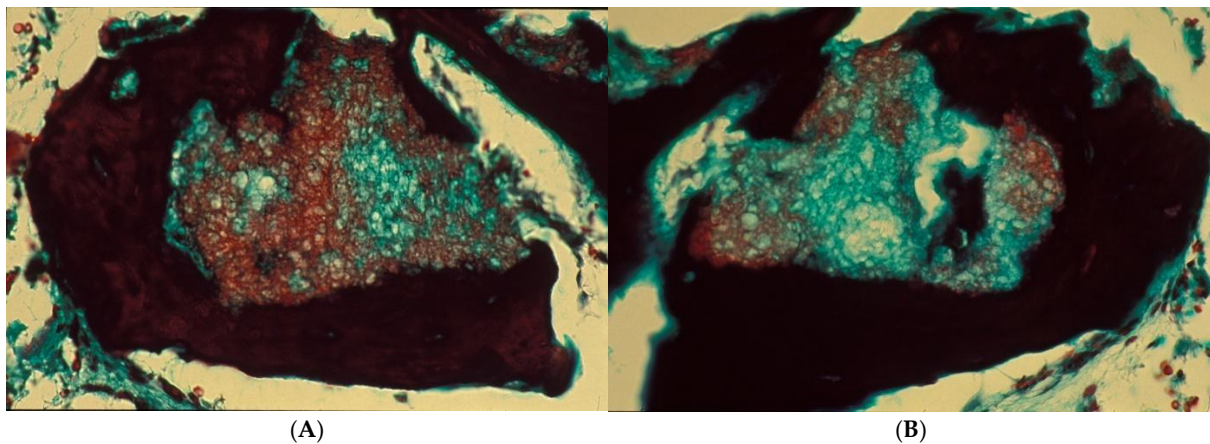


Figure 11. NH remnants were found partially or entirely enclosed in appositionally formed new bone. Azan–Mallory staining, magnification 400× (A,B).

Histologic Evaluation

Light microscopic analysis (Figure 10A–D and Figure 11A,B) revealed new bone formation throughout all parts of the biopsy, with a homogeneous presence of trabecular bone structures in intimate contact with the surface of the NH granules, and marrow spaces filled with loose, highly vascularized connective tissue. There was no evidence of inflammation or a foreign body reaction around the NH remnants, which were found partially or completely enclosed in the appositionally formed new bone.

The bone structure consisted mostly of newly formed mature lamellar bone, with Haversian systems, cement lines, and osteocytes, highlighting the vitality of the bone tissue. The non-degraded NH granules appeared structurally porous and inhomogeneous, were partially surrounded by osteoid or woven bone, and were lined with seams of osteoblasts. Osteoid protrusion and extension into the graft material were observed. Fibrovascular extension with osteoid deposition within the nanostructured porous granule was observed, which was composed of cellular fibrous connective tissue undergoing mineralization, thereby creating an arboreal network.

The presence, around the same granule, of a side with osteoclasts, as well as an osteogenic side with osteoblasts, was observed, demonstrating the integration of the biomaterial.

4. Discussion

The following four biological principles (PASS principles) have to be satisfied for a predictable and successful GBR procedure: primary wound closure for undisturbed submerged healing, angiogenesis to provide vascularization and cells, space creation and maintenance to obtain space for bone regeneration, and stability of the initial blood clot

and the particulate bone graft [3]. The physicochemical structure of biomaterials can affect their biological behavior and clinical results [6]. Although the use of autogenous bone is still considered the gold standard for graft materials, its use is limited by the availability of a proper donor site and the morbidity associated with harvesting. Allografts and xenografts are considered valid BSMs due to their osteoconductive properties. However, to remove their immunogenic proteins, these materials are processed with techniques such as irradiation or lyophilization, which are believed to decrease their regenerative qualities [8].

The majority of alloplastic BSMs are calcium phosphate-based materials. Most of the β -TCP or synthetic HA are sintered during their production phase, resulting in less porous and more compact materials, with a specific surface of below $2 \text{ m}^2/\text{g}$ and reduced osteoconductivity [9,10]. These features—including poor solubility, reduced biodegradability, and lack of phagocytability—negatively influence new bone formation, which may be disturbed, delayed, or absent, and can favor chronic inflammation [10] or sequestration [11]. Conversely, the biomaterial reported here is a non-sintered, highly porous ceramic produced by means of the sol–gel technique. In this process, a loose connection of HA nanocrystals with SiO_2 molecules occurs during the transition process from sol to gel, resulting in a nanoporously structured BSM [8]. This material is characterized by the following three types of interconnecting pores [10]: Macropores ($100 \text{ }\mu\text{m}$ – 1 mm) permit vascular tissue invasion for the proper vascularization of cellular and fibrillar elements from the initial healing phase; micropores (5 – $100 \text{ }\mu\text{m}$) allow the ingrowth of connective tissue fibers and osteoblasts, supporting a multicentric bone formation within the particles; and nanopores (2 – 10 nm) facilitates the entry of serum and plasma, promoting subsequent biodegradation and resorption [10].

The broad internal surface of NH ($84 \text{ m}^2/\text{g}$) is due to the open bonds of the silica gel [12,13], which is resorbed and substituted by an organic matrix that contains glycoproteins, complement factors, fibrinogen, and thrombocytes. Degradation of the SiO_2 gel exposes the HA particles to the angiogenic and osteogenic cells migrating into the bone defect. Silicon dioxide stimulates the formation of bone and collagen. As an essential trace element, silicon is involved in both osteoblast proliferation and connective tissue formation [12,14].

Angiogenesis is another paramount principle for GBR [3]. Osteogenesis and angiogenesis are closely coupled [15]. Blood supply is a crucial factor when using a BSM, since improper vascularization may impair osteogenesis by reducing nutrients. It is promoted by perforating the bone walls that delimit the bone defect to open the marrow cavities and encourage bleeding, which brings new vessels and undifferentiated mesenchymal cells to populate the bone defect. Proper vascularization is a vital factor for cellular colonization and appositional osteogenesis [11]. Angiogenesis is involved in successful healing and osteogenesis because the newly formed blood vessels, originating from the host vessels, enter the cavities of the NH porous granules to create an intergranular network, transporting osteoblastic precursor cells into the granules [15]. A significantly higher density of osteoclast-like cells and blood vessels was found within the regenerated area compared with the native residual bone [8].

The biodegradation and resorption of NH particles take place at the same rate as new bone formation [10] and seem to involve cellular resorption rather than enzymatic degradation [8]—through resorbing mononuclear cells, histiocytes, and macrophages in the early healing stages [11]—and Trap-positive multinucleated cells, which were demonstrated as osteoclasts or their precursors [16]. NH particles are incorporated in the remodeling process and resorbed by osteoclasts, without any histological sign of inflammation. In an *in vivo* study, osteoclastic resorption was observed at all stages investigated, revealing continuous but not excessive resorption of NH [17]. A faster resorption rate of BSM could

influence bone regenerative potential, since competing non-osteogenic cells proliferate faster than bone-forming cells and could populate the space to be regenerated. In an animal study, the histological analysis of sites grafted with β -TCP granules did not reveal any residues of the BSM. Instead, multiple foci of connective tissue with chronic inflammatory reactions were found within the newly formed bone [10]. The histological observation around the same NH particle—on one side with osteoclasts and on the other side with osteoblasts—demonstrates the biocompatibility, the tissue reaction, and the integration of the biomaterial into the physiological remodeling process of the human host [18]. In a clinical study of sinus lift procedures, only about 50% of the initially inserted NH particles were still present after about 3 months [11].

The BSM discussed in this study has osteoinductive potential and the capacity to stimulate and support the proliferation and osteogenic differentiation of mesenchymal progenitor cells in host tissue [17,19]. Grafting NH particles into ectopic tissue, such as subcutaneous adipose tissue or the muscle of sheep and mini pig, induced bone formation even after 5 weeks [17,19]. The nanostructure of this porous BSM seems to be the cause of this osteoinduction, while the replacement of the silica matrix by an organic matrix embedding proteins and growth factors is considered the key factor that triggers this process. Immunohistochemistry performed on human biopsies harvested in sinus lift procedures enabled the detection of molecules involved in osteoblast differentiation, bone mineralization and remodeling [18]. Strong immunostaining was detected for osteocalcin and osteopontin in and around the granules, as well as for BMP-2 in the NH matrix, alkaline phosphatase, collagen type 1, and vessel-like structures positive for antibodies of the von Willebrand factor [19]. The vascular endothelial growth factor, the most important angiogenic factor, was observed in bone samples from NH-augmented sites [18]. Other angiogenic factors, such as osteopontin, and hypoxia-inducible factors, which are transcription factors upregulated under hypoxic or catabolic conditions, have also been observed [15].

Immunohistochemistry utilizing the ED I antibody—a marker for cells of the mononuclear phagocyte family—showed that osteoclast precursors and macrophages were present around the vessels and within the connective tissue between the NH particles. The osteoclast-like cells were localized not only along the new bone surface but also on the NH particle [18]. Immunostaining for Runx2 detected cells in the connective tissue between the NH particles, especially around the blood vessels, demonstrating that osteoblast precursors may originate from the connective tissue from perivascular areas, thereby sustaining the osteoinductive potential of the biomaterial [18].

The use of this biomaterial has been well documented for the sinus lift procedure, with excellent results both in simultaneous implant placement [20], even after a 3-month healing time [21], and in the staged approach, which allows for histological and immunohistochemical evaluation, as a bone sample is harvested during the implant bed preparation [8,11,16,18,22–25]. It should be noted that this procedure is not considered overtreatment, as that bone would be lost anyway during surgical site preparation for the insertion of the implant. Furthermore, the histological analysis of the bone sample provides the clinician with valuable information about the degree of tissue maturation and the time required for implant osseointegration prosthetic loading.

Apart from the documentation on sinus lift procedures, few reports have been published on other types of jawbone regeneration procedures. In a localized maxillary defect, NH was used in combination with another alloplast and was covered with a titanium mesh instead of a membrane [26]. The implant was placed after a 5-month healing period in a newly formed bone that was deemed clinically hard enough, achieving good primary stability. In another study, NH granules were used to fill post-extraction sockets for an alveolar

ridge preservation procedure [27]. The graft was protected by dPTFE membranes that were intentionally left exposed to the oral cavity and were removed after 4 weeks, without the elevation of a surgical flap; they were simply lifted with tweezers. The closed structure of dPTFE membranes (0.3 μm) does not allow the passage of bacteria through the membrane, avoiding infection of the underlying bone graft [28]. Eiji Funakoshi was the first clinician to document a GBR procedure using an intentionally exposed dPTFE membrane [29], opening up new therapeutic possibilities in a field where, for years, clinicians have always strived to achieve primary wound closure through flap passivation and coronal advancement. This innovation has made the GBR procedure simpler and minimally invasive. The use of a TR-dPTFE membrane in the treatment of the current clinical case contributed to the maintenance of the space required for successful bone regeneration. The titanium frame, in addition to providing a well-defined shape to the membrane, prevented its collapse into the bone defect. Primary closure is mandatory when a resorbable membrane is used; otherwise, the barrier effect will be lost prematurely, and the bone graft may be lost and colonized by bacteria. Most resorbable membranes available on the market are mainly manufactured using collagen of animal origin—either bovine or porcine—which limits their use in countries where the use of these biomaterials is not permitted for religious reasons. This problem also exists for BSMs. In addition, for these types of biomaterials—whether of human or animal origin—also carry a risk of cross-infection [6,30].

5. Conclusions

The combination of NH and a TR-dPTFE membrane allowed for a fully synthetic GBR procedure, produced good clinical and histologic results, and represents a valid therapeutic option for the treatment of patients who, for any reason, do not accept allografts or xenografts due to their human or animal source, and who refuse to have autologous bone retrieved from another donor site. While promising, controlled histological and clinical studies are needed to confirm the results reported here.

Author Contributions: Conceptualization, F.B. and M.G.; Methodology, L.S.; Histologic Investigation, F.B.; Writing—Original Draft Preparation, F.B. and M.M.; Writing—Review and Editing, L.S., M.M. and M.G.; Supervision, M.G. and L.S.; All authors have read and agreed to the published version of the manuscript.

Funding: The authors received no external funding for writing this article.

Institutional Review Board Statement: Not applicable. Case series studies are a retrospective description of clinical findings in cases or an observed course of events that document a new aspect of patient management during the normal course of clinical treatment. In this type of study, there is no hypothesis testing, no systematic data collection beyond that which is part of routine clinical practice, no data analysis, and the clinical work has already been performed, in contrast with prospective case series. Hence, retrospective case series do not usually qualify as “research” requiring approval from ethical boards designed to protect humans involved in clinical research.

Informed Consent Statement: The patient signed an informed consent form for the whole treatment (two surgeries and prosthetic rehabilitation).

Data Availability Statement: No new data were created.

Acknowledgments: The authors wish to thank Ezio Bassotti from the Catholic University of the Sacred Heart in Rome, Italy, for processing and staining the bone biopsy, and Alessandro Nezzo for the prosthetic rehabilitation of the patient.

Conflicts of Interest: The authors declare no conflicts of interest.

References

1. Buser, D.; Dula, K.; Hess, D.; Hirt, H.P.; Belser, U.C. Localized ridge augmentation with autografts and barrier membranes. *Periodontology 2000* **1999**, *19*, 151–163. [[CrossRef](#)] [[PubMed](#)]
2. Retzepi, M.; Donos, N. Guided Bone Regeneration: Biological principle and therapeutic applications. *Clin. Oral Implants Res.* **2010**, *21*, 567–576. [[CrossRef](#)] [[PubMed](#)]
3. Wang, H.L.; Boyapati, L. “PASS” principles for predictable bone regeneration. *Implant Dent.* **2006**, *15*, 8–17. [[CrossRef](#)] [[PubMed](#)]
4. Mizraji, G.; Davidzohn, A.; Gursoy, M.; Gursoy, U.; Shapira, L.; Wilensky, A. Membrane barriers for guided bone regeneration: An overview of available biomaterials. *Periodontology 2000* **2023**, *93*, 56–76. [[CrossRef](#)]
5. Buser, D.; Urban, I.; Monje, A.; Kunrath, M.F.; Dahlin, C. Guided bone regeneration in implant dentistry: Basic principle, progress over 35 years, and recent research activities. *Periodontology 2000* **2023**, *93*, 9–25. [[CrossRef](#)]
6. Rodella, L.F.; Favero, G.; Labanca, M. Biomaterials in maxillofacial surgery: Membranes and grafts. *Int. J. Biomed. Sci.* **2011**, *7*, 81–88. [[CrossRef](#)]
7. Simion, M.; Fontana, F.; Rasperini, G.; Maiorana, C. Vertical ridge augmentation by expanded-polytetrafluoroethylene membrane and a combination of intraoral autogenous bone graft and deproteinized anorganic bovine bone (Bio Oss). *Clin. Oral Implants Res.* **2007**, *18*, 620–629. [[CrossRef](#)]
8. Ghanaati, S.; Barbeck, M.; Willershausen, I.; Thimm, B.; Stuebinger, S.; Korzinskas, T.; Obreja, K.; Landes, C.; Kirkpatrick, C.J.; Sader, R.A. Nanocrystalline hydroxyapatite bone substitute leads to sufficient bone tissue formation already after 3 months: Histological and histomorphometrical analysis 3 and 6 months following human sinus cavity augmentation. *Clin. Implant Dent. Relat. Res.* **2013**, *15*, 883–892. [[CrossRef](#)]
9. Gerike, W.; Bienengraber, V.; Henkel, K.O.; Bayerlein, T.; Proff, P.; Gedrange, T.; Gerber, T. The manufacture of synthetic non-sintered and degradable bone grafting substitutes. *Folia Morphol.* **2006**, *65*, 54–55.
10. Henkel, K.O.; Gerber, T.; Lenz, S.; Gundlach, K.K.; Bienengraber, V. Macroscopical, histological, and morphometric studies of porous bone-replacement materials in minipigs 8 months after implantation. *Oral Surg. Oral Med. Oral Pathol. Oral Radiol. Endodontology.* **2006**, *102*, 606–613. [[CrossRef](#)]
11. Mejer, J.; Wolf, E.; Bienengraber, V. Application of the synthetic nanostructured bone grafting material NanoBone® in sinus floor elevation. *Implantologie* **2008**, *16*, 301–314.
12. Gerber, T.; Traykova, T.; Henkel, K.O.; Bienengraeber, V. Development and in vivo test of sol-gel derived bone grafting materials. *J. Sol-Gel Sci. Technol.* **2003**, *26*, 1173–1178. [[CrossRef](#)]
13. Gerber, T.; Holzhueter, G.; Knoblich, B.; Doerfling, P.; Bienengraeber, V.; Henkel, K.O. Development of bioactive sol-gel material template for in vitro and in vivo synthesis of bone material. *J. Sol-Gel Sci. Technol.* **2000**, *19*, 441–445. [[CrossRef](#)]
14. Kang, Y.M.; Kim, K.H.; Seol, Y.J.; Rhee, S.H. Evaluations of osteogenic and osteoconductive properties of a non-woven silica gel fabric made by the electrospinning method. *Acta Biomater.* **2009**, *5*, 462–469. [[CrossRef](#)]
15. Götz, W.; Reichert, C.; Canullo, L.; Jäger, A.; Heinemann, F. Coupling of osteogenesis and angiogenesis in bone substitute healing—A brief overview. *Ann. Anat.* **2012**, *194*, 171–173. [[CrossRef](#)]
16. Stübinger, S.; Ghanaati, S.; Orth, C.; Hilbig, U.; Saldamli, B.; Biesterfeld, S.; Kirkpatrick, C.J.; Sader, R.A. Maxillary sinus grafting with a nano-structured biomaterial: Preliminary clinical and histological results. *Eur. Surg. Res.* **2009**, *42*, 143–149. [[CrossRef](#)]
17. Götz, W.; Lenz, S.; Reichert, C.; Henkel, K.O.; Bienengraber, V.; Pernicka, L.; Gundlach, K.K.; Gredes, T.; Gerber, T.; Gedrange, T.; et al. A preliminary study in osteoinduction by a nano-crystalline hydroxyapatite in the mini pig. *Folia Histochem. Cytobiol.* **2010**, *48*, 589–596. [[CrossRef](#)]
18. Götz, W.; Gerber, T.; Michel, B.; Lossdörfer, S.; Henkel, K.O.; Heinemann, F. Immunohistochemical characterization of nanocrystalline hydroxyapatite silica gel (NanoBone®) osteogenesis: A study on biopsies from human jaws. *Clin. Oral Implants Res.* **2008**, *19*, 1016–1026. [[CrossRef](#)]
19. Gerber, T.; Lenz, S.; Holzhueter, G.; Götz, W.; Helms, K.; Harms, C.; Mittlmeier, T. Nanostructured bone grafting substitutes—A pathway to osteoinductivity. *Key Eng. Mater.* **2012**, *493–494*, 147–152. [[CrossRef](#)]
20. Heinemann, F.; Mundt, T.; Biffar, R.; Gedrange, T.; Goetz, W. A 3-year clinical and radiographic study of implants placed simultaneously with maxillary sinus floor augmentations using a new nanocrystalline hydroxyapatite. *J. Physiol. Pharmacol.* **2009**, *60* (Suppl. 8), 91–97.
21. Canullo, L.; Patacchia, O.; Sisti, A.; Heinemann, F. Implant restoration 3 months after one stage sinus lift surgery in severely resorbed maxillae: 2-year results of a multicenter prospective clinical study. *Clin. Implant Dent. Relat. Res.* **2012**, *14*, 412–420. [[CrossRef](#)] [[PubMed](#)]
22. Canullo, L.; Dellavia, C. Sinus lift using a nanocrystalline hydroxyapatite silica gel in severely resorbed maxillae: Histological preliminary study. *Clin. Implant Dent. Relat. Res.* **2009**, *11* (Suppl. 1), e7–e13. [[CrossRef](#)] [[PubMed](#)]
23. Canullo, L.; Dellavia, C.; Heinemann, F. Maxillary sinus floor augmentation using a nano-crystalline hydroxyapatite silica gel: Case series and 3-month preliminary histological results. *Ann. Anat.* **2012**, *194*, 174–178. [[CrossRef](#)]

24. Francisco, L.; Francisco, M.; Costa, R.; Vasques, M.N.; Relvas, M.; Rajão, A.; Monteiro, L.; Rompante, P.; Guerra, F.; Infante da Câmara, M. Sinus floor augmentation with synthetic hydroxyapatite (NanoBone[®]) in combination with platelet-rich fibrin: A case series. *Biomedicines* **2024**, *12*, 1661. [[CrossRef](#)]
25. Bosshardt, D.D.; Bornstein, M.M.; Carrel, J.P.; Buser, D.; Bernard, J.P. Maxillary sinus grafting with a synthetic, nanocrystalline hydroxyapatite-silica gel in humans: Histologic and histomorphometric results. *Int. J. Periodontics Restor. Dent.* **2014**, *34*, 259–267. [[CrossRef](#)]
26. Alagl, A.S.; Madi, M. Localized ridge augmentation in the anterior maxilla using titanium mesh, an alloplast, and a nano-bone graft: A case report. *J. Int. Med. Res.* **2018**, *46*, 2001–2007. [[CrossRef](#)]
27. Laurito, D.; Cugnetto, R.; Lollobrigida, M.; Guerra, F.; Vestri, A.; Gianno, F.; Bosco, S.; Lamazza, L.; De Biase, A. Socket preservation with d-PTFE membrane: Histologic analysis of the newly formed matrix at membrane removal. *Int. J. Periodontics Restor. Dent.* **2016**, *36*, 877–883. [[CrossRef](#)]
28. Barboza, E.P.; Stutz, B.; Ferreira, V.F.; Carvalho, W. Guided bone regeneration using nonexpanded polytetrafluoroethylene membranes in preparation for dental implant placements: A report of 420 cases. *Implant Dent.* **2010**, *19*, 2–7. [[CrossRef](#)]
29. Funakoshi, E.; Yamashita, M.; Maki, K.; Kage, W.; Ishikawa, Y.; Shinichiro, H. Guided bone regeneration with Open Barrier Membrane Technique. In Proceedings of the 22nd Annual Meeting of the Academy of Osseointegration 2007, San Antonio, TX, USA, 9 March 2007.
30. Kim, Y.; Nowzari, H.; Rich, S.K. Risk of prion disease transmission through bovine-derived bone substitutes: A systematic review. *Clin. Implant Dent. Relat. Res.* **2013**, *15*, 645–653. [[CrossRef](#)]

Disclaimer/Publisher’s Note: The statements, opinions and data contained in all publications are solely those of the individual author(s) and contributor(s) and not of MDPI and/or the editor(s). MDPI and/or the editor(s) disclaim responsibility for any injury to people or property resulting from any ideas, methods, instructions or products referred to in the content.